Performance of Four Passive Microwave Soil Moisture Products in Maize Cultivation Areas of Northeast China

Xingming Zheng, *Member, IEEE*, Zhuangzhuang Feng, Hongxin Xu, Yanlong Sun, Yu Bai, Bingze Li, Lei Li, Xiaowei Zhao, Rui Zhang, Tao Jiang, *Member, IEEE*, Xiaojie Li, and Xiaofeng Li, *Member, IEEE*

***Abstract*—Passive microwave remote sensing is an effective way to obtain global soil moisture (SM) measurements, and many studies have explored the uncertainty inherent in microwave-based SM products. However, SM product accuracy has not been evaluated in northeast China, a national and global production base for commodity grain. In this study, a ground-based wireless sensor network with 28 observation nodes that were spatially distributed within 36 × 36 km was established to achieve satellite-scale "true" SM values through sensor calibration for specific soil types, senor consistency testing, and spatial scale transformation. The uncertainties of four passive microwave SM products (SMAP L3, SMOS L3, the Japan Aerospace Exploration Agency/JAXA AMSR2, and FY3C) were investigated and the following conclusions were obtained: 1) SMAP SM accuracy was very close to the expected application accuracy of 0.04 cm^3/cm^3, followed by SMOS, FY3C, and AMSR2; 2) for SMOS and SMAP, there were no significant temporal changes in SM errors, except for the larger error of descending SMOS SM and June SM values for descending SMAP and ascending SMOS. AMSR2 SM generally underestimated field SM, while FY3C SM values under low vegetation conditions were more consistent with field data, with an error of about 0.06 cm^3/cm^3; 3) agricultural activities and rainfall caused the soil surface roughness to increase or decrease within a growing season, which may have been an important source of satellite-scale SM error indicated by high bias values in July for both SMAP and SMOS; and 4) the standard deviation of field SM (0.06 cm^3/cm^3) produced a SMAP SM error of about 0.06 cm^3/cm^3 in low vegetation water content conditions, indicating that SM spatial heterogeneity cannot be ignored in the retrieval algorithm. This article investigated the accuracy and error sources of four satellite SM products in the farmland area of northeast China, and identified future research directions for further improving SM algorithms.**

***Index Terms*—China, farmland, passive microwave remote sensing, soil moisture (SM), validation.**

I. Introduction

SOIL moisture (SM) is one of the most active parameters governing water and energy cycles between the land surface and atmosphere, and it is also a key variable in hydrological, bioecological, and biogeochemical processes [1]–[4]. Long-term observations of SM over large areas are critical to many related research topics on flooding and drought monitoring, water resource management, and crop yield forecasts [5]–[8]. Passive microwave remote sensing technology can be used to monitor surface SM changes in near real time at regional and global scales due to its sensitivity to SM and ability to collect SM information under all weather conditions.

The L-band (1.4 GHz) is considered to be the best microwave frequency for obtaining surface SM because it can penetrate sparse and medium dense vegetation, and reflect deeper SM information than the C-band and X-band. With advancements in hardware and satellite technology, SM remote sensing platforms have developed to single band, low frequency L-band radiometry. The corresponding baseline algorithm for SM estimation has also developed from a multifrequency algorithm [such as the Land Parameter Retrieval Model, the Japan Aerospace Exploration Agency (JAXA) Advanced Microwave Scanning Radiometer 2 (AMSR2) algorithm, and the FY-3C/MicroWave Radiation Imager (MWRI) algorithm], to single-frequency algorithms [such as L-band Microwave Emission of Biosphere (L-MEB) for the Soil Moisture and Ocean Salinity (SMOS) satellite and Single Channel Algorithm (SCA) for the Soil Moisture Active and Passive (SMAP satellite] [9]–[16]. Based on these satellites and SM algorithms, a series of SM products have been generated using passive microwave remote sensing for agricultural, hydrological, and climate change research.

The application of microwave-based SM retrievals has been influenced and limited to some degree by the natural variability and complexity of vegetation canopies and surface roughness, which significantly affects emission measurement sensitivity to SM [17]. Validation of remotely sensed SM products is crucial

Manuscript received March 23, 2020; revised May 3, 2020 and May 14, 2020; accepted May 15, 2020. Date of publication May 19, 2020; date of current version June 4, 2020. This work was supported by the National Natural Science Foundation of China under Grant 41971323 and Grant 41771400. *(Corresponding authors: Xingming Zheng; Xiaofeng Li.)*

Xingming Zheng, Tao Jiang, Xiaojie Li, and Xiaofeng Li are with the Remote Sensing and Geographic Information System Center for Northeast Institute of Geography and Agroecology, Chinese Academy of Sciences, Changchun 130102, China (e-mail: zhengxingming@iga.ac.cn; jiangtao@iga.ac.cn; lixiaofeng@iga.ac.cn).

Zhuangzhuang Feng, Yu Bai, and Lei Li are with the School of Resources and Environment for the University of Chinese Academy of Sciences, Beijing 100049, China (e-mail: 932848240@qq.com; 937621522@qq.com; 714980196@qq.com).

Hongxin Xu and Yanlong Sun are with the Shanghai Aerospace Electronic Technology Institute, Shanghai 200092, China (e-mail: 13127726992@163.com; 14418393 @qq.com).

Bingze Li is with the School of Geomatics and Prospecing Engineering for the Jilin Jianzhu University, Changchun 130118, China (e-mail: 17600059995@qq.com).

Xiaowei Zhao is with the Institute of Economic Management Science Ministry of Natural Resources, Harbin 150081, China (e-mail: 614639191@qq.com).

Rui Zhang is with the College of Earth Exploration Science and Technology, Jilin University, Changchun 130102, China (e-mail: 137140665@qq.com).

Digital Object Identifier 10.1109/JSTARS.2020.2995623

for better understanding the errors and limitations inherent in these products, which is of great significance for further refinement and usage [18], [19]. Thus, intensive validation activities have been conducted globally for the past few years, especially in the United States [20]–[25], Europe [26]–[29], Australia [14], [30]–[33], and China [34], [35].

However, limited validation work has been performed in the Qinghai Tibetan Plateau [36]–[38], China's Heihe River Basin [39]–[44] and Genhe watershed [34]. These three regions have specific characteristics: For example, the Qinghai Tibetan Plateau site is dominated by grassland, the Genhe site is dominated by forest, and the Heihe site is dominated by mixed land cover. China's cultivated land area is 1.35×10^8 hm^2, the third largest in the world [45]. Few studies have been conducted to evaluate the accuracy and error of various passive microwave remote sensing SM products in China's farmland. It is highly affected by human activities, the surface roughness and vegetation biomass change significantly, and the SM inversion algorithm is interfered by many factors. Evaluating the uncertainty of microwave remote sensing SM products will enhance the understanding of their accuracy and facilitate their applications.

The purpose of this study is to evaluate the accuracy of passive microwave remote sensing SM products (including SM from the SMAP, SMOS, AMSR2, and FY3C satellites) in the maize area of Northeast China. In this article, the SM observation network of SM and the research area are first introduced. Then, the accuracy of passive microwave remote sensing products is evaluated. Finally, the relationship between satellite SM product errors and field SM heterogeneity is analyzed.

II. Data and Methods

A. Study Area

The location of the study area is the maize area in the north of Changchun, China, including the contiguous part of eastern of Nong'an County and western of Dehui County, where it is temperate monsoon climate with four distinct seasons. Average annual precipitation is 520 mm, mainly concentrated in July and August during summer. Average annual temperature and annual accumulated temperature are 4.4 °C and 2851 °C, respectively. The average daily temperature is below 0 °C from November to March. The frost-free period lasts about 140–150 days from May to September, which is also the crop-growing season. The research area is a representative farmland area in Northeast China, which is suitable for validating passive microwave remote sensing SM products. This area was chosen because: 1) SM validation ability needs to be improved in China's farmland area; 2) the topography is relatively flat, and the slope is between 0° and 5.8° with a standard deviation (STD) of 0.45°; 3) farmland (mainly for maize) accounts for more than 90% of pixel area and water bodies make up 0.37%; and 4) the soil texture is relatively homogeneous, and the clay and sand contents are 11.5%–12.5% and 51.5%–60.6%, respectively [46], [47].

B. SM Observation Network

The SM observation network has a spatial range of 36 × 36 km with 28 SM observation nodes. The spatial locations of SM observation nodes needed to be optimized first to make the point-scale SM better represent SM for the corresponding satellite-scale. According to the spatial distribution of soil types and soil thermal inertia related to SM, 28 SM observation nodes (Fig. 1) were selected to represent the overall SM distribution in the study area and minimize the impact of spatial heterogeneity. The footprints of four SM products (SMAP, SMOS, AMSR2, and FY3C) are shown in Fig. 1, and the number of SM observation nodes for each satellite footprint is shown in Table I. Impacted by soil freezing (November to March of the following year) and agricultural activities, SM observation nodes were set up in May of each year and removed in October to ensure that the depth of the SM sensor was in the 0–5 cm soil layer.

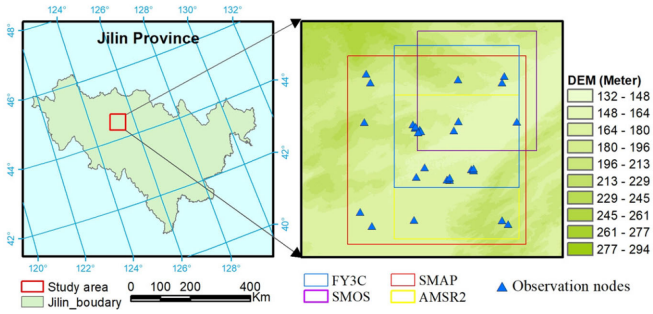

Fig. 1. Locations of SM observation nodes and the footprints of four passive microwave satellite pixels in the study area.

TABLE I
Number of SM Observation Nodes for Evaluating the Accuracy of Four Passive Microwave SM Products

Satellite	SMOS	SMAP	AMSR-2	FY-3C
Number of SM nodes	20	28	9	15

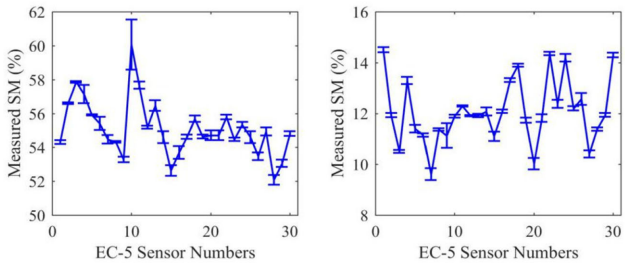

Fig. 2. Consistency comparison of observed SM results for 28 EC-5 sensors using (a) pure water and (b) dry sand at room temperature.

C. SM Sensor Installation and Calibration

An EC-5 probe made by the METER company was used to measure SM. To ensure the EC-5 sensor consistency and accuracy, we conducted a series of calibrations, including consistency tests and soil type calibration. Please refer to Fu *et al.* [47] for detailed operation steps.

Fig. 2 shows the EC-5 sensor consistency results for pure water and dry sand at 25 °C room temperature. The STD of the measured value from a single sensor was about 0.18%, which indicated that the sensor had reliable stability, except for the 11th sensor that had a pure water measurement of 1.8%. The

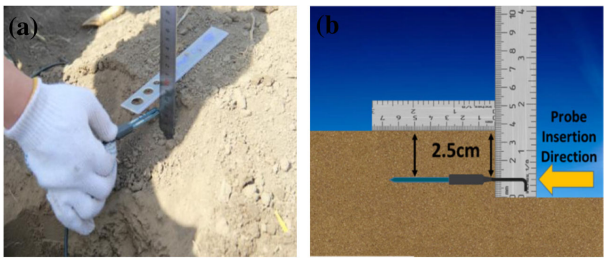

Fig. 3. Installation and arrangement of the EC-5 sensors at *in situ* points. (a) Actual sensor installation. (b) Specific installation details [47].

maximum and minimum values for pure water were 60.6% and 52.1%, respectively, an 8.5% difference. The maximum and minimum values for dry sand were 14.5% and 9.6%, a 4.9% difference. The pure water difference was higher than dry sand, possibly because EC-5 sensor uncertainty was related to the permittivity of the measured medium. The higher the permittivity, the greater the error. Generally, the dry sand results were within the $\pm 3\%$ accuracy (i.e., a 6% variation range) recommended by the sensor manufacturer, while the pure water results did not meet this range. Therefore, the consistency of all 28 sensors needed to be calibrated to ensure comparability and accuracy. In addition, the dry sand values were relatively higher than the actual values, which indicated that the EC-5 sensor may overestimate sandy soil SM and requiring sensor calibration by soil type. After these calibrations, sensor accuracy improved from 0.03 cm^3/cm^3 (factory accuracy) to 0.02 cm^3/cm^3.

All EC-5 sensors were installed at the middle of May after crop sowing and removed at the end of September before harvesting. Temporally, SM data were collected from May 10, 2017 to September 26, 2017 (corresponding to the 130th to 269th days of 2017) and from May 16, 2018 to September 26, 2018 (corresponding to the 136th to 269th days of 2018). The data were recorded once an hour. Because the farmland in the study area was characterized by ridges, EC-5 sensors were installed in ridges and ditches, and average values were used to represent the "true" value of the observed points. Sensor probes were horizontally inserted into the soil 2.5 cm from the soil surface to avoid damaging the natural vertical soil structure and ensure that the sensing depth was 0–5 cm from the soil surface. Fig. 3 shows the EC-5 sensor installation method.

D. Passive Microwave SM Products

1) SMAP SM Product: The SMAP mission, which is an L-band satellite dedicated to providing global SM at a temporal resolution of 1–3days [48], was launched by NASA on January 31, 2015. The satellite operates in a sun-synchronous orbit scanning the earth's surface in ascending (6:00 P.M.) and descending (6:00 A.M.) paths. The SMAP passive Level-3 SM product (Version 6) (L3_SM_P) has a spatial resolution of 36 km and an EASE-Grid 2.0 projection. The SMAP L3_SM_P product is freely available from the National Snow and Ice Data Center (NSIDC)[1].

V-pol SCA (SCA-V) was adopted as the operational baseline algorithm to estimate SM from SMAP brightness temperature (TB). First, the apparent emissivity was normalized from TB by surface temperatures provided by the NASA Goddard Earth Observing System Model, Version 5 (GEOS-5). By introducing the Moderate-resolution Imaging Spectroradiometer (MODIS) Normalized Difference Vegetation Index (NDVI) and the semiempirical Hp model [49] for vegetation and roughness corrections, the coupled soil and vegetation emissivity was converted to smooth bare soil. Finally, the Mironov soil dielectric model [50] and the Fresnel equation were used to relate SM with smooth bare soil emissivity. More details on the SCA-V algorithms can be found in [51].

2) SMOS SM Product: The SMOS mission is the European Space Agency's second Earth Explorer Opportunity mission and was launched on November 2, 2009. The SMOS carries a single payload, an interferometric L-band (1.4 GHz) 2-D radiometer with multiangular (0°–55°) viewing capabilities. The mission was designed for global near-surface SM (0–5 cm depth) monitoring with a temporal resolution of 2–3 days [52]. The satellite orbits the earth at a local overpass time of 6:00 A.M. (ascending) and 6:00 P.M. (descending). In the operational SMOS retrieval algorithm, SM and vegetation optical depth were simultaneously retrieved based on SMOS multiangular and dual-polarization TB, and the L-MEB model was used as the forward model [53]. Surface temperatures derived from the European Centre for Medium-Range-Weather Forecasts (ECMWF) were used for surface temperature correction. The retrieval process was based on an iterative approach that minimizes a cost function calculated from the weighted sum of square deviations between the measured and modeled TB for a variety of incidence angles and polarizations [54].

The SMOS products used here were the Level 3 SM (SMOS L3, Version 3.00) products from the Centre National d'Etudes Spatiales and the Centre Aval de Traitement des Données SMOS (CNES/CATDS), with an EASE-Grid 2.0 projection and a 25-km spatial resolution. The SMOS L3 SM dataset was downloaded from CATDS (available at ftp://ftp.ifremer.fr). In this study, two filters were considered for excluding unreliable SMOS-L3 data with a Data Quality Index value greater than 0.1 (Soil_Moisture_ Dqx > 0.1) and a radio frequency interference (RFI) probability greater than 0.2 (RFI_Prob>0.2) [34], [55]. More details on the SMOS-L3 retrieval algorithm can be found in [54].

3) JAXA AMSR2 SM Product: The AMSR-2 is a passive microwave sensor on board the Global Change Observation Mission for Water-1 (GCOM-W1) satellite, which was launched by JAXA in May 2012. The AMSR-2 is the successor of the successful AMSR-E (May 2002 to October 2011). The AMSR-2 is a conical-scanning microwave imager with 14 channels at the following seven frequencies: 6.925, 7.3, 10.65, 18.7, 23.8, 36.5, and 89.0 GHz. The local crossing times are approximately 1:30 P.M. and 1:30 A.M. for ascending and descending overpasses, respectively [56], [57].

The JAXA AMSR2 Level 3 0.25° global grid SM product data were acquired at the GCOM-W1 Data Providing Service[2]. The

[1][Online]. Available: https://nsidc.org/ data/SPL3SMP

[2][Online]. Available: https://gcom-w1.jaxa.jp/auth.html

JAXA algorithm uses a forward radiative transfer scheme to calculate TBs for multiple frequencies and polarizations according to different vegetation and soil conditions. SM was estimated using a lookup table based on the results and the polarization ratio at 10.65 GHz and index of soil wetness at the 36.5 and 10.65 GHz horizontal channels [56], [58].

4) FY3C/MWRI L2 SM Product: FY3C/MWRI Level 2 EASE-Grid SM product data were acquired from the FENGYUN Satellite Data Center[3]. In this study, the daily dataset of ascending (10:00 P.M.) and descending (10:00 A.M.) orbit with a spatial resolution of 25 km was used. The current FY-3C SM retrieval algorithm is a radiative transfer-based model that links SM, land surface temperature, and vegetation optical depth to 10.65 GHz H/V channels TB observed by the MWRI [59]. A parameterized surface emission model (the Qp model) [60] for bare surface and the empirical relationship between NDVI and vegetation water content (VWC) used to estimate vegetation optical depth [61] were adopted for roughness and vegetation correction. Finally, the dielectric mixing model proposed by Wang and Schmugge [62] and the Fresnel equation were used to convert soil emissivity to SM.

E. Error Metrics

The thiessen polygon method adopted for SMAP SM validation [41] was used to upscale point-based field SM to pixel-based SM, to reduce the uncertainty of validation caused by the spatial mismatch between ground observations and satellite results. The thiessen polygon method was carried out based on a Matlab code by combining spatial location of SM observing points and the boundary of satellite footprint. The modified SM time-series was compared with the four satellite SM products (SMAP, SMOS, AMSR2, and FY3C), and four indices (root mean square error—*RMSE*, unbiased *RMSE*—*ubRMSE*, mean bias—*Bias*, and Pearson's correlation coefficient—*R*) were used to assess the satellite SM product accuracy. They are defined as follows [48]:

$$\text{Bias} = E\left[SM_{\text{SAT}}\right] - -E\left[SM_{\text{Field}}\right] \tag{1}$$

$$\text{RMSE} = \left[E(SM_{\text{SAT}} - -SM_{\text{Field}})^2\right]^{0.5} \tag{2}$$

$$ub\text{RMSE} = \left(\text{RMSE}^2 - -\text{Bias}^2\right)^{0.5} \tag{3}$$

$$R = \text{Cov}\left(SM_{\text{SAT}}, SM_{\text{Field}}\right) / \left[\text{Var}\left(SM_{\text{SAT}}\right) \cdot \text{Var}\left(SM_{\text{Field}}\right)\right] \tag{4}$$

where SM_{SAT} and SM_{Field} are the satellite-based SM and the upscaled field SM, respectively, E[·] and Var (·) represent the average value and variance of a data set. Cov(X, Y) is the covariance of X and Y.

III. Results

A. Temporal and Spatial Characteristics of Field SM

Due to seasonal frozen soil and human activities, field SM measurements were taken for 2017 and 2018 from May to September. There were 140 days with field SM measurements in 2017 and 134 in 2018. Fig. 4 shows the average SM values at all measurement points in the study area and the corresponding daily rainfall data provided by ECWMF[4]. Average SM from May to October was 0.215 cm^3/cm^3, with respective maximum and minimum values of 0.294 and 0.065 cm^3/cm^3, respectively. Maximum daily rainfall was about 60 mm. Fig. 4 shows that rainfall and SM had a good corresponding relationship. Rainfall events greater than 10 mm corresponded to a significant increase in SM, confirming the reliability of field SM.

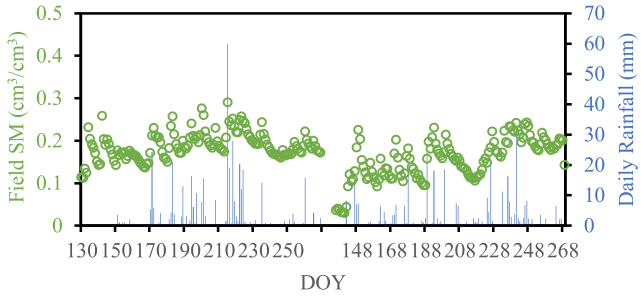

Fig. 4. Temporal change of average values of field SM from 28 observation nodes and daily rainfall from European Centre for Medium-Range Weather Forecasts (ECMWF) during 2017–2018.

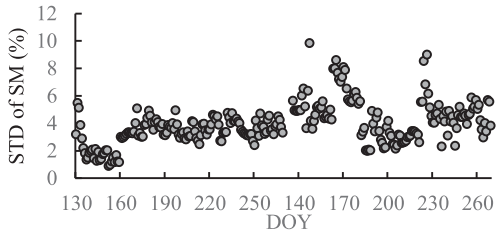

Fig. 5. STD of field SM with observation time.

Fig. 5 shows the temporal variability of field SM STD. The maximum and minimum STD values were 9.85% and 0.9% respectively, with an average of 3.93%. The STD for SSM between the 150th and 180th days in 2018 was relatively high, because it was relatively dry in this period and some farmers irrigated their maize fields, resulting in the increase of spatial heterogeneity.

B. Accuracy of the Four Passive Microwave SM Products

Fig. 6 compares field SM values and satellite SM results estimated from SMAP, SMOS, FY3C, and AMSR2 TB.

In general, the SMAP SM temporal variability was in good agreement with field SM. The R, Bias, RMSE, and ubRMSE results between the ascending SMAP SM and field values were 0.45, 0.029, 0.062, and 0.055 cm^3/cm^3, respectively, while the corresponding results for descending SMAP SM were 0.48, −0.005, 0.051, and 0.051 cm^3/cm^3 (Table II). The statistical results showed that SMAP SM accuracy in ascending orbit was better than in descending orbit. However, Fig. 6 shows that there was no obvious difference between ascending and descending

[3][Online]. Available: http://satellite.nsmc.org.cn/

[4][Online]. Available: http://apps.ecmwf.int/datasets/data/interim-full-aily/levtype=sfc/

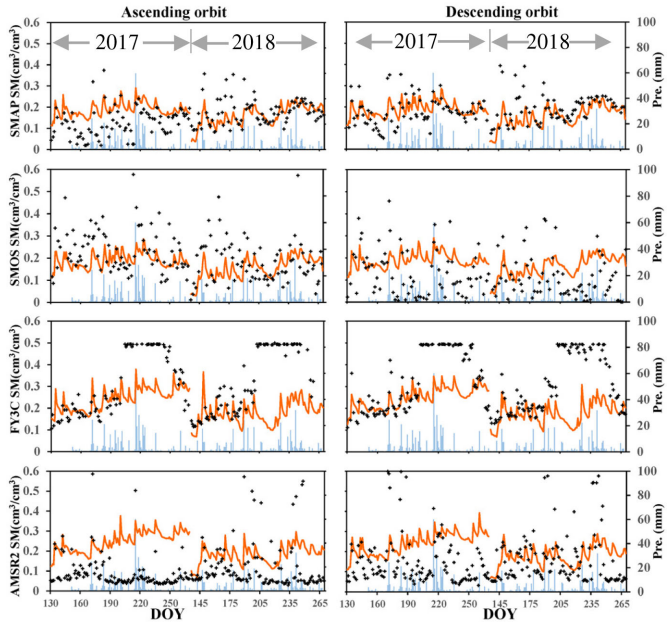

Fig. 6. Comparison of upscaled field SM and estimated SM values from SMAP, SMOS, FY3C, and AMSR2. The red line represents the field SSM, gray "+" represents satellite-based SM, and green bar represents daily rainfall from ECWMF.

TABLE II
ERROR (R, RMSE, BIAS, AND UBRMSE) RESULTS OF FOUR PASSIVE MICROWAVE REMOTE SM PRODUCTS (SMAP, SMOS, FY3C, AND AMSR2)

SATELLITE		SMAP	SMOS	FY3C	AMSR2
ASCENDING	*R*	0.45	0.20	0.3800	0.1100
	RMSE	0.062	0.1433	0.1929	0.1421
	Bias	0.029	0.0503	0.1343	0.0924
	ubRMSE	0.055	0.1341	0.1385	0.1079
DESCENDING	*R*	0.48	0.19	0.3100	0.0900
	RMSE	0.051	0.1163	0.1758	0.1347
	Bias	-0.005	0.0578	0.1182	0.0378
	ubRMSE	0.051	0.1009	0.1301	0.1293

SMAP SM values, so the differences in statistical accuracy may have resulted from SM overestimation during/after rainfall. Overall, SMAP and field SM consistency during the later period of vegetation growth was higher than during sowing. This temporal difference in SMAP SM accuracy may have been related to surface roughness, vegetation, and their heterogeneity.

The *R* between SMOS L3 SM and field SM was approximately 0.2. Respective bias, RMSE, and ubRMSE values for the ascending overpass were 0.0503, 0.143 cm^3/cm^3, and 0.1431, and 0.0204 cm^3/cm^3, 0.064, and 0.0607 cm^3/cm^3 for the descending overpass. There was better consistency between the ascending SMOS SM and field SM results than the descending results, which clearly underestimated SM.

The *R*, *Bias*, *RMSE,* and *ubRMSE* values for the ascending FY3C SM were 0.38, 0.1343, 0.1929, and 0.1385 cm^3/cm^3, respectively, and 0.31, 0.1182, 0.1758, and 0.1301 cm^3/cm^3 for the descending results. After the 220th day of each year (i.e., when VWC $\approx$ 3 kg/m^2), the retrieved SM was almost saturated because the X-band could not penetrate the vegetation to sense the change in SM. This resulted in lower overall SM accuracy. If we only considered VWC less than 3 kg/m^2, the bias of ascending (descending) FY3C SM decreased from 0.1343 (0.1182 cm^3/cm^3) to -0.0329 cm^3/cm^3 (-0.0310 cm^3/cm^3), which meant that low vegetation conditions produced high accuracy. In addition, *R* and *RMSE* also improved. The *R* for ascending (descending) FY3C SM improved from 0.3802 (0.3075) to 0.3884 (0.4327), and the *RMSE* for ascending (descending) FY3C SM decreased from 0.1929 (0.1785 cm^3/cm^3) to 0.0750 cm^3/cm^3 (0.0695 cm^3/cm^3), which was also close to the desired accuracy of 0.06 cm^3/cm^3.

R, *Bias*, *RMSE*, and *ubRMSE* values for ascending AMSR2 SM were 0.11, 0.0924, 0.1421 and 0.1079 cm^3/cm^3, respectively, and 0.09, 0.0378, 0.1347, and 0.1293 cm^3/cm^3 for the descending results. The AMSR2 JAXA SM products generally underestimated field SM. Except for rainfall, only small fluctuations were observed for the temporal AMSR2 JAXA SM. These two issues have been confirmed by previous studies [34], [47]. AMSR2's X-band TB is used to estimate SM in the JAXA SM algorithm, and its penetration ability is relatively weak compared with the L-band. It can only detect SM from shallower surfaces.

IV. DISCUSSION

The uncertainty of SM estimated by microwave remote sensing is caused by many factors, including: 1) the mismatch in SM sensing depth and spatial scale of *in situ* SM and satellite observations [18], [63]; 2) the possible errors in ground measurements; 3) the effects of RFI probability; and 4) the inaccurate parameterization of the input factors of the SM retrieval algorithm (e.g., surface temperature, vegetation, and surface roughness) in the SM retrieval algorithm [64], [65]. Here, the error sources were investigated by analyzing the effect of the temporal change (mainly surface roughness and vegetation), RFI probability, uncertainties of soil temperature and spatial heterogeneity in field SM on satellite-based SM results.

A. Temporal Change in Passive Microwave SM Product Error

The two main factors that affect the accuracy of SM products are vegetation canopy and soil surface roughness, which are time-varying parameters for farmland surfaces within a year. To evaluate error sources of SM product, we analyzed the temporal distribution of SM errors from May to September (Fig. 7).

The JAXA AMSR2 and FY3C algorithms use the X-band TB to estimate SM, both of which have weak penetrability. In the later crop growth period, they can hardly penetrate vegetation to detect changes in surface SM. Therefore, their accuracy during the later growth period (July, August, and September) is significantly lower than in the early period of crop growth (May and June). Here, their accuracy in May and June was compared with *in situ* SM, and the FY3C SM products had higher accuracy than AMSR2 (Fig. 7).

Both the SMAP and SMOS missions are equipped with L-band microwave radiometers, but with different imaging methods and SM algorithms. Overall, the accuracy of their SM products was better than AMSR2 and FY3C. From May to September, the precision of the SMAP SM products was almost the same for ascending and descending orbits. For ascending

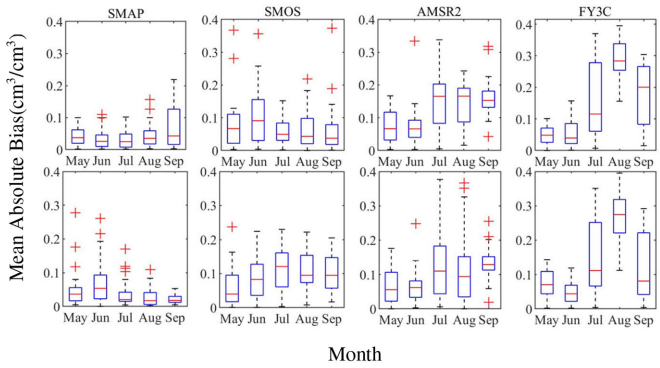

Fig. 7. Temporal changes of mean absolute bias for four SM products (SMAP, SMOS, AMSR2, and FY3C). The top figures are for ascending orbit, and the bottom figures are for descending orbit.

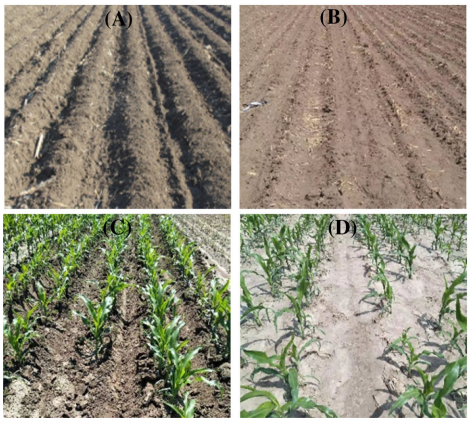

Fig. 8. Bare and vegetated soil surface with different roughness affected by farming activities and natural conditions. (a) Soil surface with a ridge structure. (b) Soil surface with no tillage cultivation. (c) Vegetated soil surface with farming activities. (d) Vegetated soil surface without farming activities.

orbit, bias during August and September was higher than in the other three months. For descending orbit, the bias was high in June. The bias of the ascending and descending SMOS SM products differed greatly from May to September, and the ascending orbit bias was less than the descending bias. A high bias occurred in June for ascending orbit and in July for descending orbit. High bias occurred when the surface roughness changed (in June and July, for example) or when the VWC was high (as in August and September) for both the SMAP and SMOS SM products.

In this study area, May and June corresponded to the sowing and seedling stages, and crop VWC was relatively low. The estimated SM error was mainly attributed to surface roughness and SM spatial and vertical heterogeneity. Surface roughness related to human activities may have had a greater impact on SM error. These errors may have originated from two factors: 1) the difference in initial roughness caused by cultivation techniques, such as traditional ridge cultivation [Fig. 8(a)] where there are ridges, and no tillage cultivation where no ridges are present [Fig. 8(b)]; and 2) the change in surface roughness over time due to rainfall and farming activities. Rainfall significantly reduces surface roughness of newly plowed soil, and the root mean

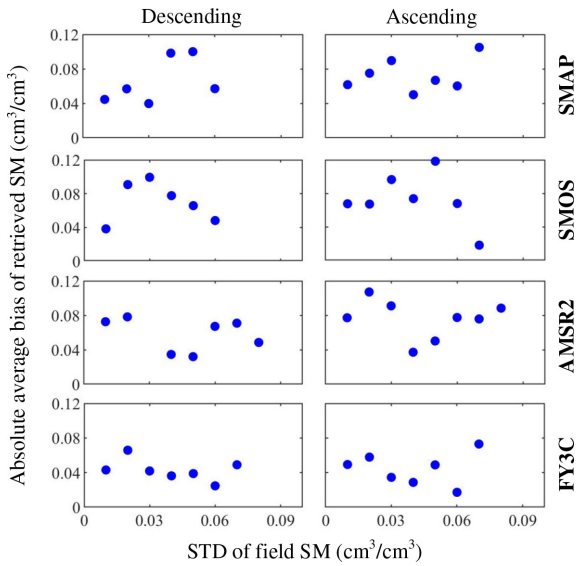

Fig. 9. Relationship between the STD of field SM and the mean bias of four satellite-based SM (SMAP, SMOS, AMSR2, and FY3C).

square height is reduced to half of its initial value during May to September [63]. Generally, in the middle of June (when the height of corn was about 30–40 cm), some farmers began to fertilize corn for improving yields, and this mechanized operation significantly damaged the original soil surface and increased surface roughness [Fig. 8(c) and (d)]. This showed that soil surface roughness varied over time [66], [67]. In the SMAP and SMOS SM baseline algorithms, however, surface roughness does not change with time, which is bound to introduce some uncertainties into SM products. This effect was obvious around the 160th–170th day of 2017 for SMAP SM products when the increase in soil surface roughness led to the underestimation of SM. However, it is difficult to obtain a quantitative description of temporal changes in soil surface roughness, and research on this change will be an important aspect for improving satellite SM product accuracy.

B. Effect of SM Spatial Heterogeneity on SM Accuracy Evaluation Results

SM spatial heterogeneity is an important error source of satellite-based SM. There are many factors affecting spatial heterogeneity, including rainfall, vegetation, topography, soil type, and so on. In this article, we did not analyze the causes of spatial heterogeneity, but rather the relationship between spatial heterogeneity and satellite-based SM error. Here, SM spatial heterogeneity within a microwave pixel was represented by the STD of field SM. Estimated SM accuracy in the later stage of vegetation growth was easily affected by vegetation. To reduce the impacts of vegetation canopy on the results, only data from May to July were selected to analyze the relationship between STD of field SM and satellite-based SM error, shown in Fig. 9. There was a reliable positive correlation between the STD and SMAP SM error for both ascending and descending orbits, with R-square values around 0.6. Field SM STD changed from 0.01

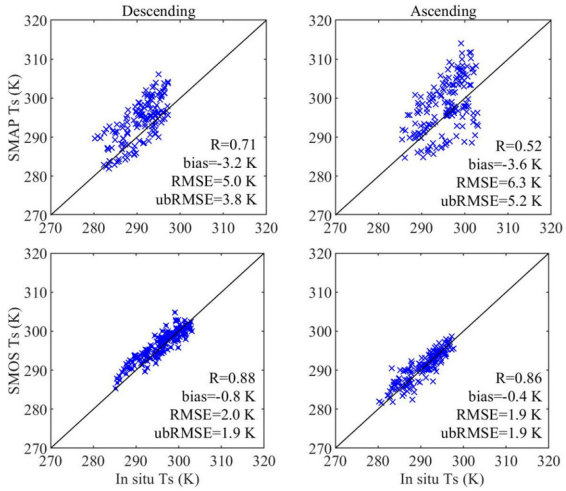

Fig. 10. Comparison of *in situ* soil temperature and soil temperature used in the SMAP and SMOS algorithms.

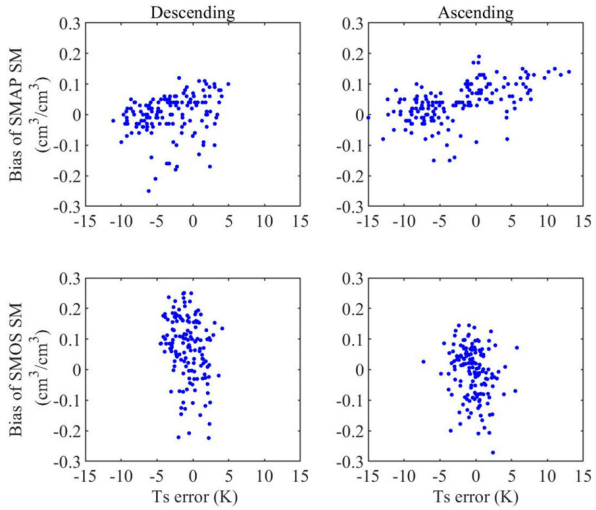

Fig. 11. Scatter diagram of surface temperature (Ts) error and bias of satellite-based SM bias.

to 0.07 cm^3/cm^3, and the corresponding average absolute error of SMAP SM increased from 0.04 to nearly 0.10 cm^3/cm^3. SM STD variability and the average absolute error of SMAP SM were both about 0.06 cm^3/cm^3, and this similar change range also confirmed the dependence of SMAP SM error on STD of field SM.

This correlation between SMOS SM error and SM STD could also be found when SM STD is smaller than 0.03 and 0.05 cm^3/cm^3 for descending and ascending orbits, respectively. But there was no relationship between AMSR2 (and FY3C) SM error and SM STD. This could be explained in two ways: 1) the accuracy of SMAP SM was higher than that of other three products; and 2) the observation sites in SMAP footprint were more than that of other three satellites, and the STD of field SM could better express the spatial heterogeneity of SM. Nevertheless, it could be inferred that the SM spatial heterogeneity might affect the satellite-based SM accuracy for farmland in northeast China, which needed to be included in the future SM retrieval algorithms.

C. Effect of Uncertainties of Surface Temperature Used in SMAP and SMOS on SM Accuracy Evaluation Results

The SMAP surface temperature (SMAP Ts) was predicted from the NASA GEOS-5 model, and SMOS surface temperature (SMOS Ts) was obtained from the ECMWF model. The comparison results of SMAP Ts and SMOS Ts with *in situ* Ts (Fig. 10) indicated that the error of SMAP Ts was greater than that of SMOS Ts due to its low R and high RMSE. In other words, the consistency between SMOS Ts and *in situ* Ts was better than SMAP Ts. Also, there was a positive correlation between SMAP Ts error and the bias of SMAP SM (Fig. 11). It was consistent with the previous research results [65], [68], that is, the overestimation (or underestimation) of Ts lead to the overestimation (or underestimation) of estimated SM. Fig. 11 also showed that there was no obvious relationship between SMOS Ts error and SMOS SM bias, because SMOS Ts error is relatively small and the error of SMOS SM was mainly affected by factors other than Ts.

D. Effect of RFI Probability on SM Accuracy Evaluation Results

RFI was also the main error source of retrieved SM from the L-band TB. In order to reduce the influence of RFI, SMAP satellite increased the sampling frequency of microwave radiometer, and divided the bandwidth of 24 MHz into 16, 1.5 MHz subbands. In each subband and the total band, various methods (time-domain pulse detection, cross frequency detection, kurtosis detection, and polarization characteristic analysis) were used to detect and filter RFI, which greatly improves the quality of L-band TB [69]. SMOS did not design the RFI detection unit on the satellite, which led to the unavailability of TB in some parts of the world. Subsequently, researchers did a lot of ground work to detect and suppress RFI, but small-scale RFI could not be fully identified. These RFI residues will affect the accuracy of SMOS SM products. Thus, annual average RFI probability of SMOS TB was computed for both ascending and descending orbits, and the RFI probability of P.M. Orbit (34.1%) was higher than that of A.M. orbit (19.9%) for SMOS. This explained to a certain extent why the error of the descending (P.M.) SMOS SM was greater than that of the ascending (A.M.) orbit.

V. Conclusion

Using SM-measured data from a ground wireless observation network, this article evaluated the uncertainty of four passive microwave remote sensing SM products (SMAP, SMOS, AMSR2, and FY3C) in the farmland area of northeast China, and the change in SM uncertainty across seasons (observation time). The effects of spatial heterogeneity, RFI-contaminated probability and surface temperature uncertainty on satellite-scale SM product error were also discussed. Some conclusions are as follows.

A SM observation network with 28 observation nodes was established for measuring SM in a maize cultivation area of northeast China. After sensor consistency testing and soil type calibration, the SM senor accuracy was about 0.02 cm^3/cm^3. This network provided a reliable ground data set for evaluation.

Compared to upscaled field SSM, the accuracy of SMAP satellite SM product was the highest, followed by SMOS, FY3C, and AMSR2. Pearson correlation coefficient (R) for ascending and descending SMAP SM products with field SSM were 0.45 and 0.48 respectively, and the corresponding bias results were 0.029 and -0.005 cm^3/cm^3. R values for SMOS and field SM were about 0.2 for both ascending and descending orbits, and their ubRMSE results were about 0.1 cm^3/cm^3. R values for AMSR2 SM and field SM decreased, and AMSR2 SM underestimated actual SM. FY3C SM was able to detect SM changes when the VWC was less than 3 kg/m^2. In general, the RMSE values of SMAP and SMOS SM are higher than 0.04 cm^3/cm^3, while those of AMSR2 and FY3C SM are higher than 0.06 cm^3/cm^3, indicating that their respective precision failed to meet the designed precision requirements for the northeast farmland area.

Farming activities and rainfall cause temporal change in the surface roughness of farmland in northeast China within one growth cycle; for example, surface roughness increases due to sowing and decreases due to rainfall. The SMAP and SMOS SM baseline algorithms assumed the roughness factor remained constant, which introduced uncertainty into SM estimates.

There was a correlation between SMAP SM error and spatial heterogeneity of SM within a microwave pixel, but this relationship is not true for SMOS, AMSR2, and FY3C. The reason might be that the field SM could better reflect the spatial heterogeneity of the SMAP footprints and the precision of SMAP SM was better than other three SM results.

The accuracy of SMOS Ts was higher than that of SMAP Ts, and there is a good correlation between SMAP Ts error and SMAP SM bias for this study area. The RFI probability of P.M. orbit was higher than that of A.M. orbit for both SMOS and SMAP, and it was one of reasons why the SM error of the descending SMOS was greater than that of the ascending (A.M.) orbit.

ACKNOWLEDGMENT

The authors would like to thank the Changchun Jingyuetan remote sensing test site and the Chinese Academy of Sciences for providing ground soil moisture data.

REFERENCES

[1] T. J. Schmugge, P. Gloersen, T. Wilheit, and F. Geiger, "Remote sensing of soil moisture with microwave radiometers," *J. Geophys. Res.*, vol. 79, no. 2, pp. 317–323, Feb. 1974.

[2] H. Douville and F. Chauvin, "Relevance of soil moisture for seasonal climate predictions: A preliminary study," *Climate Dyn.*, vol. 16, no. 16, pp. 719–736, Oct. 2000.

[3] E. Daly and A. Porporato, "A review of soil moisture dynamics: From rainfall infiltration to ecosystem response," *Environ. Eng. Sci.*, vol. 22, no. 1, pp. 9–24, Jan. 2005.

[4] J. C. Shi *et al.*, "Progress on microwave remote sensing of land surface parameters," *Sci. China Earth Sci.*, vol. 55, no. 7, pp. 1052–1078, Jul. 2012.

[5] R. Bindlish, W. T. Crow, and T. J. Jackson, "Role of passive microwave remote sensing in improving flood forecasts," *IEEE Geosci. Remote Sens. Lett.*, vol. 6, no. 1, pp. 112–116, Jan. 2009.

[6] J. D. Bolten, W. T. Crow, X.W. Zhan, T. J. Jackson, and C. A. Reynolds, "Evaluating the utility of remotely sensed soil moisture retrievals for operational agricultural drought monitoring," *IEEE J. Sel. Topics Appl. Earth Observ. Remote Sens.*, vol. 3, no. 1, pp. 57–66, Mar. 2010.

[7] R. Saini, G. L. Wang, and J. S. Pal, "Role of soil moisture feedback in the development of extreme summer drought and flood in the United States," *J. Hydrometeorology*, vol. 17, no. 8, pp. 2191–2207, Jun. 2016.

[8] S. I. Seneviratne *et al.*, "Investigating soil moisture climate interactions in a changing climate: A review," *Earth Sci. Rev.*, vol. 99, no. 3, pp. 125–161, May 2010.

[9] H. Yang and J. C. Shi, "On the estimation of land surface parameters by using FY-3A microwave radiometer imager (MWRI)," *Remote Sens. Technol. Appl.*, vol. 20, no. 1, pp. 194–200, 2005.

[10] E. G. Njoku, T. J. Jackson, V. Lakshmi, T. K. Chan, and S. V. Nghiem, "Soil moisture retrieval from AMSR-E," *IEEE Trans. Geosci. Remote Sens.*, vol. 41, no. 2, pp. 215–229, Mar. 2003.

[11] K. Imaoka *et al.*, "Five years of AMSR-E monitoring and successive GCOM-W1/AMSR2 instrument[C]," in *Proc. SPIE 6744, Sensors, Syst., Next- Gener. Satellites XI*, vol. 6744. Florence, Italy: SPIE, 2007, Art. no. 67440J.

[12] J. P. Wigneron *et al.*, "L-band microwave emission of the biosphere (L-MEB) model description and calibration against experimental data sets over crop fields," *Remote Sens. Environ.*, vol. 107, no. 4, pp. 639–655, Apr. 2007.

[13] H. Yang *et al.*, "The FengYun-3 microwave radiation imager on-orbit verification," *IEEE Trans. Geosci. Remote Sens.*, vol. 49, no. 11, pp. 4552–4560, Nov. 2011.

[14] P. O'Neill *et al.*, *Algorithm Theoretical Basis Document Level 2 & 3 Soil Moisture (Passive) Data Products[R]. JPL D- 66480*. Pasadena, CA, USA: Jet Propulsion Laboratory, 2016.

[15] R. Fernandez-Moran *et al.*, "SMOS-IC: An alternative SMOS soil moisture and vegetation optical depth product," *Remote Sens*., vol. 9, no. 5, May 2017, Art. no. 457.

[16] Y. C. Zhu *et al.*, "Evaluation of Fengyun-3C soil moisture products using in-situ data from the chinese automatic soil moisture observation stations: A case study in henan province, China," *Water*, vol. 11, no. 2, Jan. 2019, Art. no. 248.

[17] T. Koike, E. Njoku, T. J. Jackson, and S. Paloscia, "Soil moisture algorithm development and validation for the ADEOS-II/AMSR," in *Proc. IEEE Geosci. Remote Sens. Symp. (IGARSS)*, vol. 3, 2000, pp. 1253–1255.

[18] J. Y. Zeng, Z. Li, Q Chen, H. Y. Bi, J. X. Qiu, and P. F. Zou, "Evaluation of remotely sensed and reanalysis soil moisture products over the Tibetan plateau using in-situ observations," *Remote Sens. Environ.*, vol. 163, pp. 91–110, Apr. 2015.

[19] H. L. Ma *et al.*, "Satellite surface soil moisture from SMAP, SMOS, AMSR2 and ESA CCI: A comprehensive assessment using global ground-based observations," *Remote Sens. Environ.*, vol. 231, pp. 91–110, 2019.

[20] T. W. Collow, A. Robock, J. B. Basara, and B. G. Illston, "Evaluation of SMOS retrievals of soil moisture over the central United States with currently available *in situ* observations," *J. Geophys. Res.*, vol. 117, pp. D09113, May, 2012.

[21] D. J. Leroux *et al.*, "Comparison between SMOS, VUA, ASCAT, and ECMWF soil moisture products over four watersheds in US," *IEEE Trans. Geosci. Remote Sens.*, vol. 52, no. 3, pp. 1562–1571, Jan. 2013.

[22] T. W. Ford, C. O. Wulff, and S. M. Quiring, "Assessment of observed and model-derived soil moisture-evaporative fraction relationships over the United States southern great plains," *J. Geophys. Res. Atmos.*, vol. 119, pp. 6279–6291, Jun. 2014.

[23] K. C. Kornelsen, M. H. Cosh, and C. Paulin, "Potential of bias correction for downscaling passive microwave and soil moisture data," *J. Geophys. Res. Atmos.*, vol. 120, pp. 6460–6479, Jul. 2015.

[24] S. K. Chan *et al.*, "Assessment of the SMAP passive soil moisture product," *IEEE Trans. Geosci. Remote Sens.*, vol. 54, no. 8, pp. 4994–5007, Aug. 2016.

[25] X. F. Zhang, T. T. Zhang, P. Zhou, Y. Shao, and S. Gao, "Validation analysis of SMAP and AMSR2 soil moisture products over the United States using ground-based measurements," *Remote Sens*., vol. 9, no. 2, Jan. 2017, Art. no. 104.

[26] H. Mittelbach, F. Casini, I. Lehner, A. J. Teuling, and S. I. Seneviratne, "Soil moisture monitoring for climate research: Evaluation of a low cost sensor in the framework of the Swiss soil experiment (Swiss SMEX) campaign," *J. Geophys. Res.*, vol. 116, pp. D05111, Mar. 2011.

[27] N. Pierdicca, L. Pulvirenti, R. Crapolicchio, M. Talone, and F. Fascetti, "Analysis of two years of ASCAT and SMOS derived soil moisture estimates over Europe and North Africa," *Eur. J. Remote Sens.*, vol. 46, no. 6, pp. 759–773, Dec. 2013.

[28] S. Kim, Y. Y. Liu, F. M. Johnson, R. M. Parinussa, and A. Sharma, "A global comparison of alternate AMSR2 soil moisture products: Why do they differ?," *Remote Sens. Environ.*, vol. 161, pp. 43–62, Feb. 2015.

[29] A. Gruber, C. H. Su, W. T. Crow, S. Zwieback, W. A. Dorigo, and W. Wagner, "Estimating error cross-correlations in soil moisture data sets using extended collocation analysis," *J. Geophys. Res. Atmos.*, vol. 121, no. 3, pp. 1208–1219, Feb. 2016.

[30] R. Panciera, J. P. Walker, J. D. Kalma, E. J. Kim, K. Saleh, and J. P. Wigneron, "Evaluation of the SMOS L-MEB passive microwave soil moisture retrieval algorithm," *Remote Sens. Environ.*, vol. 113, no. 2, pp. 435–444, Feb. 2009.

[31] C. S. Draper, J. P. Walker, P. J. Steinle, R. A. M. D. Jeu, and T. R. H. Holmes, "An evaluation of AMSR-E derived soil moisture over Australia," *Remote Sens. Environ.*, vol. 113, no. 4, pp. 703–710, Apr. 2009.

[32] M. S. Yee, J. P. Walker, A. Monerris, C. Rüdiger, and T. J. Jackson, "On the identification of representative in situ soil moisture monitoring stations for the validation of SMAP soil moisture products in Australia," *J. Hydrol*, vol. 537, pp. 367–381, Jun. 2016.

[33] E. Cho, C. H. Su, D. Ryu, H. Kim, and M. Choi, "Does AMSR2 produce better soil moisture retrievals than AMSR-E over Australia?," *Remote Sens. Environ.*, vol. 188, pp. 95–105, Jan. 2017.

[34] H. Z. Cui *et al.*, "Evaluation and analysis of AMSR-2, SMOS, and SMAP soil moisture products in the Genhe area of China," *J. Geophy. Res. Atmos.*, vol. 122, Aug. 2017, doi: 10.1002/2017JD026800.

[35] Q. Liu, J. Y. Du, J. C. Shi, and L. M. Jiang, "Analysis of spatial distribution and multi-year trend of the remotely sensed soil moisture on the Tibetan Plateau," *Sci. China Earth Sci.*, vol. 56, no. 12, pp. 2173–2185, Dec. 2013.

[36] Z. Su *et al.*, "The Tibetan plateau observatory of plateau scale soil moisture and soil temperature (Tibet-Obs) for quantifying uncertainties in coarse resolution satellite and model products," *Hydrol. Earth Syst. Sci.*, vol. 15, pp. 2303–2316, Jul. 2011.

[37] B. Su, P. D. Rosnay, J. Wen, L. S. Wang, and Y. J. Zeng, "Evaluation of ECMWF's soil moisture analyses using observations on the Tibetan plateau," *J. Geophys. Res. Atmos.*, vol. 118, pp. 5304–5318, Jun. 2013.

[38] Y. Y. Chen, K. Yang, J. Qin, L. Zhao, W. J. Tang, and M. L. Han, "Evaluation of AMSR-E retrievals and GLDAS simulations against observations of a soil moisture network on the central tibetan plateau," *J. Geophys. Res. Atmos.*, vol. 118, no. 10, pp. 4466–4475, May 2013.

[39] D. Z. Li, R. Jin, J Zhou, and J. Kang, "Analysis and reduction of the uncertainties in soil moisture estimation with the L-MEB Model using EFAST and ensemble retrieval," *IEEE Geosci. Remote Sens. Lett.*, vol. 12, no. 6, pp. 1337–1341, Feb. 2015.

[40] Z. Lu, L. N. Chai, T. Zhang, H. Z. Cui, and W. J. Li, "AMSR2 retrievals using observation of soil moisture network on the upper and middle reaches of Heihe river basin," *Remote Sens. Tec. Appl.*, vol. 32, no. 2, pp. 324–337, 2017.

[41] C. F. Ma, X. Li, L. Wei, and W. Z. Wang, "Multi-Scale validation of SMAP soil moisture products over cold and arid regions in northwestern China using distributed ground observation data," *Remote Sens.*, vol. 9, no. 4, Mar. 2017, Art. no. 327.

[42] A. Colliander *et al.*, "Validation of SMAP surface soil moisture products with core validation sites," *Remote Sens. Environ.*, vol. 191, pp. 215–231, Mar. 2017.

[43] R. Jin *et al.*, "A nested ecohydrological wireless sensor network for capturing the surface heterogeneity in the midstream areas of the Heihe river basin, China," *IEEE Geosci. Remote Sens. Lett.*, vol. 11, no. 11, pp. 2015–2019, Nov. 2014.

[44] X. Li *et al.*, "Heihe watershed allied telemetry experimental research (HIWATER): Scientific objectives and experimental design," *Bull. Amer. Meteorol. Soc.*, vol. 9, no. 8, pp. 1145–1160, Aug. 2013.

[45] Y. J. Chen, X. Y. Yi, L. N. Fang, and R. Z. Yang, "Analysis of cultivated land and grain production potential in China," *Scientia Agricultura Sinica*.,vol. 49, no. 6, pp. 1117–1131, Jun. 2016.

[46] X. M. Zheng, Y. Bai, T. Jiang, X. Zhao, and K. Zhao, "Evaluation of SMAP L2/L3 passive soil moisture products using *in-situ* data from a dense observation network over agricultural area in northeast China," in *Proc. IEEE Geosci. Remote Sens. Symp.*, 2018, pp. 6949–6952.

[47] H. Y. Fu, T. T. Zhou, and C. L. Sun, "Evaluation and analysis of AMSR2 and FY3B soil moisture products by an in situ network in cropland on pixel scale in the northeast of China," *Remote Sens.*, vol. 11, no. 7, Apr. 2019, Art. no. 868.

[48] D. Entekhabi *et al.*, "The Soil Moisture Active Passive (SMAP) mission," *Proc. IEEE*, vol. 98, no. 5, pp. 704–716, Jun. 2010.

[49] B. Choudhury, T. J. Schmugge, A. Chang, and R. Newton, "Effect of surface roughness on the microwave emission from soils," *J. Geophys. Res. Oceans.*, vol. 84, pp. 5699–5706, 1979.

[50] V. L. Mironov, L. G. Kosolapova, and S. V. Fomin, "Physically and mineralogically based spectroscopic dielectric model for moist soils," *IEEE Trans. Geosci. Remote Sens.*, vol. 47, no. 7, pp. 2059–2070, Aug. 2009.

[51] P. E. O'Neill, S. Chan, E. Njoku, T. J. Jackson, and R. Bindlish, *Algorithm Theoretical Basis Document (ATBD): L2/3_SM_P*. CA, USA: Jet Propulsion Laboratory NASA, 2015.

[52] Y. H. Kerr, P. Waldteufel, J. P. Wigneron, J. Martinuzzi, J. Font, and M. Berger, "Soil moisture retrieval from space: The soil moisture and ocean salinity (SMOS) mission," *IEEE Trans. Geosci. Remote Sens.*, vol. 39, no. 8, pp. 1729–1735, Sep. 2001.

[53] J. P. Wigneron *et al.*, "Modelling the passive microwave signature from land surfaces: A review of recent results and application to the L-band SMOS & SMAP soil moisture retrieval algorithms," *Remote Sens. Environ.*, vol. 192, pp. 238–262, Mar. 2017.

[54] Y. K. Kerr *et al.*, "The SMOS soil moisture retrieval algorithm," *IEEE Trans. Geosci. Remote Sens.*, vol. 50, no. 5, pp. 1384–1403, May 2012.

[55] H. Lievens *et al.*, "SMOS soil moisture assimilation for improved hydrologic simulation in the Murray Darling Basin, Australia," *Remote Sens. Environ.*, vol. 168, pp. 146–162, Oct. 2015.

[56] T. Maeda *et al.*, "Status of GCOM-W1/AMSR2 development, algorithms, and products," *SPIE Remote Sens*., vol. 8176, pp. 6012–6015, Oct. 2011.

[57] M. Kachi, M. Hori, T. Maeda, and K. Imaoka, "Status of validation of AMSR2 on board the GCOM-W1 satellite," in *Proc. IEEE Geosci. Remote Sens. Symp. (IGARSS)*, Quebec, Canada, 2014, pp. 110–113.

[58] H. Fujii, T. Koike, and K. Imaoka, "Improvement of the AMSR-E algorithm for soil moisture estimation by introducing a fractional vegetation coverage dataset derived from MODIS data," *J. Remote Sens. Soc. Japan*, vol. 29, pp. 282–292, 2009.

[59] R. J. Sun, Y. P. Zhang, and J. Y. Du, "The application of FY3/MWRI soil moisture product in the summer drought monitoring of middle China," in *Proc. IEEE. Geosci. Remote Sens. Symp. (IGARSS)*, Beijing, China, 2016, pp. 2967–2969.

[60] J. C. Shi, L. M. Jiang, L. X. Zhang, K. S. Chen, J. P. Wigneron, and A. Chanzy, "A parameterized multifrequency-polarization surface emission model," *IEEE Trans. Geosci. Remote Sens.*, vol. 43, no. 12, pp. 2831–2841, Jun. 2005.

[61] T. J. Jackson *et al.*, "Soil moisture mapping at regional scales using microwave radiometry: The southern great plains hydrology experiment," *IEEE Trans. Geosci. Remote Sens.*, vol. 37, no. 5, pp. 2136–2151, Sep. 1999.

[62] J. R. Wang and T. J. Schmugge, "An empirical model for the complex dielectric permittivity of soils as a function of water content," *IEEE Trans. Geosci. Remote Sens.*, vol. 18, no. 4, pp. 288–295, Nov. 1980.

[63] A. Al-Yaari *et al.*, "Global-scale evaluation of two satellite-based passive microwave soil moisture datasets (SMOS and AMSR-E) with respect to land data assimilation system estimates," *Remote Sens. Environ.*, vol. 149, pp. 181–195, 2014.

[64] J. Zeng *et al.*, "A preliminary evaluation of the SMAP radiometer soil moisture product over United States and Europe using ground-based measurements," *IEEE Trans. Geosci. Remote Sens.*, vol. 54, no. 8, pp. 4929–4940, Aug. 2016.

[65] C. Cui *et al.*, "Soil moisture mapping from satellites: An intercomparison of SMAP, SMOS, FY3B, AMSR2, and ESA CCI over two dense network regions at different spatial scales," *Remote Sens.*, vol. 10, no. 1, 2018, Art. no. 33.

[66] X. Zheng *et al.*, "The temporal variation of farmland soil surface roughness with various initial surface states under natural rainfall conditions," *Soil Tillage Res.*, vol. 170, pp. 147–156, Jul. 2017.

[67] X. Zheng *et al.*, "Temporal evolution characteristics and prediction methods of spatial correlation function shape of rough soil surfaces," *Soil Tillage Res.*, vol. 195, Dec. 2019, Art. no. 104417.

[68] Q. Chen *et al.*, "Soil moisture retrieval from SMAP: A validation and error analysis study using ground-based observations over the Little Washita Watershed," *IEEE Trans. Geosci. Remote Sens.*, vol. 56, no. 3, pp. 1394–1408, Mar. 2018.

[69] J. R. Piepmeier *et al.*, "Radio-frequency interference mitigation for the soil moisture active passive microwave radiometer," *IEEE Trans. Geosci. Remote Sens.*, vol. 52, no. 1, pp. 761–775, Jan. 2014.

Xingming Zheng (Member, IEEE) received the Ph.D. degrees in cartography and geographic information system from the Northeast Institute of Geography and Agroecology, Chinese Academy of Sciences, Changchun, China, in 2012.

Since July 2012, he is a Research Associate with the Northeast Institute of Geography and Agroecology, Chinese Academy of Sciences. His research interests include passive microwave remote sensing of soil moisture, geophysical inversion model, microwave radiative/scattering transfer model and its application on crop canopy.

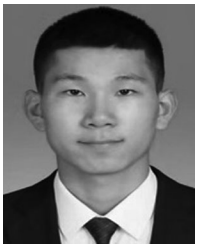

Zhuangzhuang Feng received the B.S. degree in surveying and mapping engineering from the Shandong University of Technology, Zibo, China, in 2019. Since September 2019, he has been working toward the M.S. degree with the Northeast Institute of Geography and Agroecology, Chinese Academy of Sciences, Changchun, China.

His research interests include passive/active microwave remote sensing of soil moisture, geophysical inversion model, and agricultural remote sensing.

Hongxin Xu received the bachelor's degree in radio physics from East China Normal University, Shanghai, China, in 2001.

Since July 2001, he has been a Researcher with the Shanghai Aerospace Electronic Technology Institute, Shanghai, China. His research interests include microwave radiometer systems, microwave radar systems, and instrument calibration.

Yanlong Sun received the master's degree from Shanghai Aerospace Technology Research Institute, Shanghai, China, in 2014.

Since April 2014, he has been an Engineer with Shanghai Aerospace Electronics Technology Institute. His research interests include active passive remote sensing and system design.

Yu Bai received the master's degrees in cartography and geographic information system from Jilin University, Changchun, China, in 2018. Since September 2018, he has been working toward the Ph.D. degree in cartography and geographic information system from the State Key Laboratory of Remote Sensing Science, Aerospace Information Research Institute, Chinese Academy of Sciences, Beijing, China.

His research focuses on passive microwave remote sensing inversion of soil moisture.

Bingze Li (Member, IEEE) received the bachelor's degree in surveying and mapping engineering from Jilin Jianzhu University, Changchun, China, in 2019.

Since May 2018, he has been jointly trained with the Northeast Institute of Geography and Agroecology, Chinese Academy of Sciences, Changchun, China. His research interests include passive microwave remote sensing of soil moisture and the manufacture of soil moisture sensor.

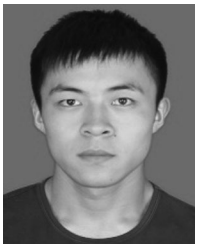

Lei Li (L, IEEE) received the master's degree in surveying and mapping engineering from the College of Geoexploration Science and Technology, Jilin University, Changchun, China, in 2018. Since September 2019, he has been working toward the Ph.D. degree with the Northeast Institute of Geography and Agroecology, Chinese Academy of Sciences, Changchun, China.

His research interests include agricultural remote sensing, hydrological models, data assimilation, and unmanned aerial vehicle agricultural remote sensing.

Xiaowei Zhao received the master's degree in cartography and geographic information engineering from Jilin University, Changchun, China, in 2019.

Since July 2019, he has been an Assistant Engineer with the Institute of Economic Management Science, Ministry of Natural Resources. His research interests include active microwave remote sensing of soil moisture, geophysical inversion model, and algorithm and data processing.

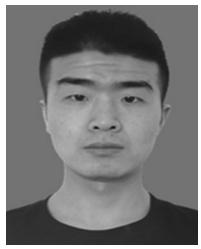

Rui Zhang (Member, IEEE) received the master's degree in geological engineering from Jilin University, Changchun, China, in 2020.

Since April 2018, it has been jointly cultivated in Northeast Institute of Geography and Agroecology, Chinese Academy of Sciences, Changchun, China. His research interests include active microwave remote sensing of soil moisture and quantitative remote sensing of vegetation.

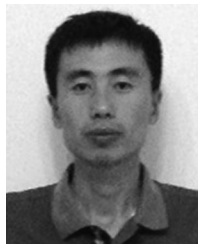

Tao Jiang (Member, IEEE) received the Ph.D. degree in cartography and geographic information system from Northeast Institute of Geography and Agroecology, Chinese Academy of Sciences, Changchun, Jilin, China, in 2019.

He is currently an Engineer with the Microwave Remote Sensing Group, Research Center of Remote Sensing and Geoscience, Northeast Institute of Geography and Agroecology, Chinese Academy of Sciences. His research interests include microwave radiometer design and the development and detection of radio freqeuncy interference.

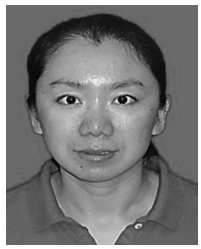

Xiaojie Li (Member, IEEE) received the Ph.D. degree in optical engineering from Tianjin University, Tianjin, China, in 2010.

Currently, she is an Associate Professor with the Northeast Institute of Geography and Agroecology, Chinese Academy of Sciences, China. Her research interests include photoelectric detection technology and remote sensing data processing and high performance computing.

Xiaofeng Li (Member, IEEE) received the B.Sc. and M.Sc. degrees in mathematics from Jilin University, Changchun, China, in 2002 and 2005, respectively, and his Ph.D. degree in remote sensing and geosciences from the Chinese Academy of Sciences, Changchun, China, in 2008.

Currently, he is a Professor with the Research Center of Remote Sensing and Geoscience, Northeast Institute of Geography and Agroecology, Chinese Academy of Sciences. His research interests include land surface parameters inversion by remote sensing data, image processing, and data analysis.

Dr. Li is the Chair of IEEE GRSS Changchun Chapter. He has published more than 50 papers in journals and conference proceedings.